

We are IntechOpen, the world's leading publisher of Open Access books Built by scientists, for scientists

5,300

Open access books available

130,000

International authors and editors

155M

Downloads

Our authors are among the

154

Countries delivered to

TOP 1%

most cited scientists

12.2%

Contributors from top 500 universities



WEB OF SCIENCE™

Selection of our books indexed in the Book Citation Index
in Web of Science™ Core Collection (BKCI)

Interested in publishing with us?
Contact book.department@intechopen.com

Numbers displayed above are based on latest data collected.
For more information visit www.intechopen.com



Advances in Derivative Voltammetry - A Search for Diagnostic Criteria of Several Electrochemical Reaction Mechanisms

Myung-Hoon Kim

Abstract

New methods for analysis of current-potential curves in terms of their derivatives are presented for studying various types of electrode processes – such as simple electron transfer reactions (reversible, quasi-reversible, and irreversible electron transfer) as well as chemically coupled electron transfer reactions along with a diagnostic scheme for differentiating these various types of electrochemical reaction mechanisms. Expressions for first- and higher order derivatives are derived from theoretical analytical solutions for currents for the different types of electrode mechanisms. The derivative curves are analyzed in terms of various parameters which characterize *peak shape or peak symmetry* with an emphasis on *the second derivatives* with well-defined anodic and cathodic peaks. Second derivatives can yield, in a simpler manner, the symmetry ratios; i.e., a ratio of anodic to cathodic peak-currents (i_p^a/i_p^c), and a ratio of anodic to cathodic peak-widths (W_p^a/w_p^c) and a ratio of anodic to cathodic peak potential differences ($\Delta E_p^a/\Delta E_p^c$) or a peak separation ($E_p^a-E_p^c$) are evaluated, and these ratio can be related to kinetic parameters associated with a particular types of electrode mechanisms. Peaks are found to be symmetrical for a simple reversible electron transfer process (E_r). However, peaks *become asymmetrical* when the electron transfer become slower (namely, irreversible, E_{irr}) or e^- transfer reaction is coupled with homogeneous chemical reactions such as a prior reaction (CE_r) or a follower-up reaction (EC_r). From measured values of such symmetry ratios above, one can gain insight to the nature of the electrochemical systems enabling us to determine various kinetic parameters associated with a system. A diagnostic criteria for assigning a electron mechanism is devised based on the values of asymmetry parameters measured, which are unity for a simple reversible electron transfer process.

Keywords: Derivative Voltammetry, Electrochemical Reaction Mechanism, Electrode Kinetics, Reversible, Quasi-reversible, and Irreversible Electron Transfer, Chemically Couple Electron Transfer, Diagnostic Criteria for Electrode Processes

1. Introduction

The aim of this Chapter is several folds (1) to provide a brief background on the derivative approach in measurements and its various applications in science and

engineering fields, (2) to review some of our research work on advances on derivatives voltammetry (DV) which have been scattered among dozens of different journals and conference presentations/proceedings in the past, together with additional new findings and development which have not been published yet, (3) to analyze and compare those characteristic results from each of different electrochemical reaction mechanisms, and to construct a master table of diagnostic criteria for differentiating various types of the electrode mechanisms. Namely, as the subtitle indicates, the primary goal of the project is, utilizing derivative voltammetry, to invent a general criteria for differentiating various types of electrode processes, in order to complement other methods such as cyclic voltammetry(CV), which is the most popular one, or Cyclic Square-Wave Voltammetry (CSWV).

1.1 Backgrounds

Derivatives approaches in analyzing data signals, have attracted much interests producing numerous research articles in the past [1–32]. Although earlier pioneering reports on the derivative approach in electrochemistry are found in the reference sections in our previous reports in electroanalytical chemistry [11–15], the approach with derivatives is not only limited to electrochemical methods but also have extended to other various fields of science and engineering [23–27, 33]. These reviews and earlier articles introduces basics of the method and techniques of signal processing [2–4, 28, 34], as applied to spectroscopic and spectrophotometric data [2–9, 34], electrochemical data [10–21], and other signals from seismic data [23] and data from biomechanics measurements [24–27, 33]. Several group [3, 6] extended the derivatives to as high as to fourth order for enhanced peak resolutions. For example, a single broad peak of UV absorption spectrum from a ternary mixture of amino acids (phenylalanine, tyrosine and tryptophan), were separated and resolved in its second and fourth derivatives [3]; the physiological states of certain algae have been assessed from an analysis of 4th derivative of absorption spectra of chlorophyll a and b [6]; a second order derivatives of an IR spectra of a DNA in malignant tissues exhibits some differences from those of a normal one [7]. The ever increasing interests in the derivative approaches in analysis of signals stem from (a) the information hidden behind in the raw data can be easily exposed from analysis of finer features emerged in the shapes of derivatives, the higher order the more the revelation, and (b) the technical advances in digital signal enhancing methods [2, 14, 15, 23–29, 34] that improve the S/N ratio which was not possible from analog instruments. A review of signal processing in electrochemistry with an introduction of software packages and extensive references therein by Jakubowska [29] may provide further assistance for interested readers.

In the field of electrochemical analysis, the derivative approach has been applied to potentiometric [10, 16] as well as to voltammetric measurements [10–22] with the enhanced resolution and better signal-to-noise (S/N) ratios.

More recent applications for derivative techniques have also been reported for analysis of oxidation of methanol [21], for improved quantification of ill-defined peaks in determining Pt in water and sediments [35], for analysis of alloxan [36], and for quantitation of naringin, an antioxidant [37].

1.2 Application to study of electrochemical reaction mechanisms

Most reports of derivative approach on electrochemical system has been for its application in chemical analysis [10, 19, 20] while only few groups have attempted to apply the approach to the study of kinetics of electrode reactions [11–18, 21, 22]. Elucidation of electrochemical reaction mechanisms on electrode surface is not only

important in developing electroanalytical methods for determining an analyte in a system but also devising effective electrochemical energy storage cells and other applied fields of engineering.

1.2.1 Drawbacks of cyclic voltammetry

As far as method of studying electrode reaction mechanisms concerned [1, 38], the cyclic voltammetry (CV) has been dominant in the field [39–41]. However, we have developed this new derivative approach to investigate electrode kinetics [11–15] in order to help in elucidating electrochemical reaction mechanisms: this is because CV has drawbacks of complications arising from the interference of the capacitive current to charge the electrical double layer at the interface; as results those peaks from CV are not purely Faradaic, and giving problems associated with defining/evaluation peak currents (i_p), and peak potentials (E_p) and peak widths (W_p). In present work, currents are taken in normal pulse voltammetric (NPP) mode by sampling the current near the end of a pulse in order to minimize the non-Faradaic currents: then, first-, second-, and third- derivatives are taken from the NPP data.

1.2.2 Several common types of electrochemical systems

The electrochemical systems under present investigation includes the simple electron transfer process; the reversible electron transfer reaction (E_r type of mechanism), and quasi-reversible (E_{quasirev} type) and irreversible (E_{irr} type) electron transfer [11, 15], and chemically coupled e^- transfer processes with a prior chemical equilibrium (CE_r type) [12, 13, 42] as well as those with a post-kinetic process (E_rC type) [14] all on a planar electrode. The observed currents may be influenced by the heterogeneous kinetic constants for an electron transfer reactions (*i.e.*, the transfer coefficient, α , and heterogeneous rate constant, k^0) for E_{irr} and E_{quasirev} type of processes [15], as well as the homogeneous rate constant (k) and equilibrium constant (K_{eq}) for E_rC or CE_r type of processes [13, 14]. In this study, the effects of these various kinetic variables on the current and its derivatives are also investigated.

1.2.3 Experimental measurements of derivatives

The theoretical voltammogram (zeroth-order derivative) is basically to emulate a normal pulse voltammogram (NPV) obtained with a normal pulse mode from an electrochemical analyzer with a DME or HMDE or SMDE (static mercury drop electrode) [11]; typically, with a pulse period of 1.000 s, pulse width of 50 ms, current sampling time of 33 ms, and scan rate of 1 mV/sec or 2 mV/s with a commercial electrochemical analyzer such an instrument as BAS-100 and Tacussel PRG-5 Pulse Polarograph. In calculation of theoretical currents, the original currents are normalized by dividing them with the diffusion controlled current (i_d) to obtain a dimensionless currents.

1.3 Basic scheme with symmetry in the peaks associated with derivative voltammetry and definitions of various parameters from the plots of currents and its derivatives

Please refer to the **Figure 1** for the definitions of all the dependent variables associated with the current-potential curve (zeroth order derivative) and its first, second and third derivatives. All measured variable and derived variables associated

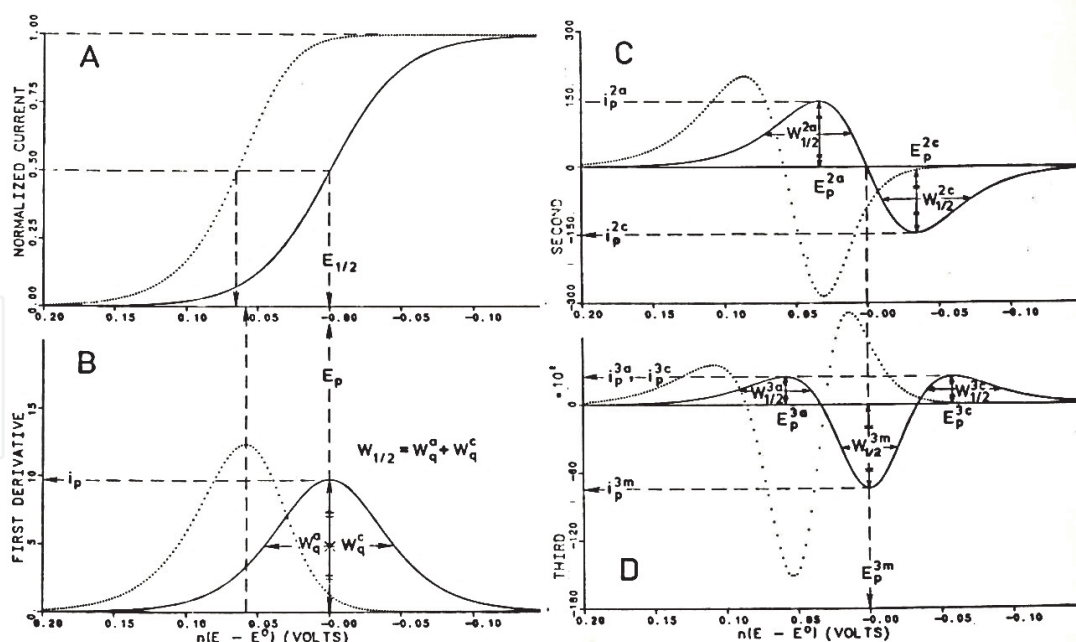


Figure 1.

Normal pulse voltammograms (A) and their higher order derivatives: 1st order (B), 2nd order (C), and 3rd derivatives (D). Several important experimental variables (parameters) such as peak-potentials, peak-currents and peak-widths are defined on the graph, for two different electrode mechanisms; (1) for a simple E_{rev} type mechanism (solid lines), and (2) for a reversible electron transfer coupled with a follow-up chemical reaction (E_rC type of mechanism). Potentials (x-axis) are with respect to a formal potential, E^0 , or $E_{1/2}$ for the E_{rev} reaction. Calculated for $T = 298\text{ K}$ and $t = 0.952\text{ s}$. the currents are normalized with respect to the diffusion currents and dimensionless; thus, the unit of first derivatives is V^{-1} , second derivatives is V^{-2} , third derivatives is V^{-3} . Note: For the original currents (A), only the half-wave potential ($E_{1/2}$) is graphically defined. Graphic definitions of the quarter-wave potential ($E_{1/4}$) and three-quarter-wave potential ($E_{3/4}$), are omitted in order to make the figure simple.

with current and the derivatives are listed in **Table 1** along with those values for a reversible e- transfer process, which is the most simple type [15].

1.3.1 Symmetry parameters

A quantitative measure of symmetry in the original current are not readily available, but can be found indirectly (and inconveniently) from a ratio of difference in several potentials defined from an original voltammogram (zeroth order derivatives): namely, a quarter-wave potentials ($E_{1/4}$, at which a current reaches a quarter of the diffusion current, i_d), half-wave potentials ($E_{1/2}$ or E_h) and a three-quarter-wave potentials, $E_{3/4}$, at which a current becomes $(3/4)i_d$; then a ratio of an anodic to cathodic quarter-wave potential differences from a half-wave potentials (i.e., $\Delta E_q^a / \Delta E_q^c = (E_{1/2} - E_{1/4}) / (E_{1/2} - E_{3/4}) = R_q^0$) is calculated. It is very limited.

However, measurements of symmetry parameters from the first derivatives are much easier than those from the original current, yielding a variety of (half a dozen) of variables. Namely, in addition to that based on peak potential differences (with respect to E^0), a peak current, half-peak width and anodic and cathodic and quarter-peak widths, and a ratio of anodic to cathodic quarter-peak width ($R_w^1 = W_q^a / W_q^c$) are also available. The second derivative can be characterized by more (about ten) variables, such as peak potentials and their ratio ($R_{\Delta E}^2 = \Delta E_p^{2a} / \Delta E_p^{2c}$), peak currents and their ratio ($R_i^2 = |i_p^{2a} / i_p^{2c}|$), and half-peak widths and a ratio of anodic to cathodic half-peak widths ($R_w^2 = W_{1/2}^{2a} / W_{1/2}^{2c}$). For the third derivative, with appearance of an additional third peak, the number of variables doubles to about twenty: three peak potentials, the differences among them, and

	Parameters	Definitions	E_r	Parameters	Definitions	E_r
<i>Current</i>			<i>3rd Der.</i>			
	$E_{1/4}$ (mV)		+28	E_p^{3a} (mV)		59
	$E_{1/2}$ (mV)		0	E_p^{3m} (mV)		0.00
	$E_{3/4}$ (mV)		-28	E_p^{3c} (mV)		-59
	ΔE_q^a (mV)	$E_{1/4}-E_{1/2}$	28	ΔE_p^3 (mV)	$E_p^{3a}-E_p^{3c}$	118
	ΔE_q^c (mV)	$E_{1/2}-E_{3/4}$	28	ΔE_a^3 (mV)	$E_p^{3a}-E_p^{3m}$	59
	ΔE_h^0 (mV)	$E_{1/4}-E_{3/4}$	56.4	ΔE_c^3 (mV)	$E_p^{3m}-E_p^{3c}$	59
	R_q^0	$\Delta E_q^a/\Delta E_q^c$	1.0	$R_{\Delta E^3}$	$\Delta E^{3a}/\Delta E^{3c}$	1.00
<i>1st Der.</i>				i_p^{3a}		2461
	ΔE_p^1 (mV)	E_p-E^0	0.0	i_p^{3m}		-7382
	R_i^1	i_p/i_d	9,7	i_p^{3c}		2461
	$W_{1/2}$ (mV)		90.5	R_i^3	i_p^{3a}/i_p^{3c}	1.00
	W_q^a (mV)		45.3	R_i^{3a}	$ i_p^{3a}/i_p^{3m} $	0.32
	W_q^c (mV)		45.3	R_i^{3c}	$ i_p^{3c}/i_p^{3m} $	0.32
	R_w^1	W_q^a/W_q^c	1.00	$W_{1/2}^{3a}$ (mV)		54
<i>2nd Der.</i>				$W_{1/2}^{3m}$ (mV)		41
	E_p^{2a} (mV)		34	$W_{1/2}^{3c}$ (mV)		54
	E_p^{2c} (mV)		-34	R_w^3	$W_{1/2}^{3a}/W_{1/2}^{3c}$	1.00
	E_p^2 (mV)	$E_p^{2a}-E_p^{2c}$	68	R_w^{3a}	$W_{1/2}^{3a}/W_{1/2}^{3m}$	1.32
	$R_{\Delta E^2}$	$\Delta E_p^{2a}/\Delta E_p^{2c}$	1.00	R_w^{3c}	$W_{1/2}^{3c}/W_{1/2}^{3m}$	1.32
	i_p^{2a}		14			
	i_p^{2c}		-14			
	R_i^2	$ i_p^{2a}/i_p^{2c} $	1.00			
	$W_{1/2}^{2a}$ (mV)		64			
	$W_{1/2}^{2c}$ (mV)		64			
	R_w^2	$W_{1/2}^{2a}/W_{1/2}^{2c}$	1.00			

Table 1. Definitions of original and derived parameters and the values for the simple reversible e^- transfer reaction. Calculated for $n = 1$ and at 298 K.

three peak currents and their ratios, and three half-peaks widths and their ratios. Among the ratios from third derivative, the ratio of anodic to cathodic peak potential difference ($R_{\Delta E^3} = \Delta E^{3a}/\Delta E^{3c}$), the anodic to cathodic peak currents ratio ($R_i^3 = i_p^{3a}/i_p^{3c}$), and a ratio of anodic to cathodic half-peak widths ($R_w^3 = W_{1/2}^{3a}/W_{1/2}^{3c}$) are most notable. All of these ratios are particularly noticeable being utilized as symmetry parameters: and *all of these values of symmetry parameters are unity (1.00) for an E_r type*. Unlike E_r that exhibits a well-defined perfect symmetry in the derivative curves, these parameter values become no longer unity for other type of slower electron transfer mechanisms (E_{irr} , and $E_{quasirev}$) or a fast e^- transfer reaction (E_{rev}) is chemically coupled homogeneously (namely, CE_r and E_rC type), introducing *asymmetry* in those curves.

As far as analysis of *the derivatives* concerned, most of the work have dealt with only the linear diffusion (on a planar electrode) or semi-infinite liner diffusion (on DME, or SMDE), not with spherical diffusion (on a spherical electrode), even

though there are many studies on the original currents (not derivatives) with spherical electrodes from earlier days of polarographic/voltammetric works as given in general monographs [30, 38, 43, 44] as well as in articles on particular systems and methods [45–55]. These include studies on EC mechanisms [45, 46], CE mechanisms [46, 47, 54], on various pulse polarographic methods [48, 55], on DC polarography [49], on AC polarography [72], on cyclic voltammetry [51], on catalytic EC mechanism with the square-wave voltammetry [52], on a double potential method [53] and on DPV at spherical and microelectrodes [56].

1.3.2 Effects of electrode sphericity

Current-potentials curves depends not only on types of the electrode mechanisms but also shape (geometry) of electrodes. However, present study focuses on a planar electrode with a linear diffusion. The effect of electrode sphericity can be minimized on planar electrode in pulse or ultrafast voltammetry because the diffusion layer thickness near the electrode is also depend on the duration of the applied potentials [43]: with application of short pulses, diffusion onto a spherical electrode (for cases with DME, HMDE, and SMDE) is approximated to a linear diffusion by minimizing the diffusion layer thickness, Nevertheless, effects of electrode sphericity *on the derivatives* of currents have been addressed by other groups [18, 54, 56] and author's group [31, 32]. Recently, Molina and coworkers [18] took a different approach that examine the dependence of peak-potentials (E_p) and peak-currents (i_p) in first derivatives on the dimensionless rate constant ($\chi = k\tau$) and on the dimensionless electrode sphericity ($\xi = (Dt)^{1/2}/r$); and found that, as the sphericity increases, the peak-potentials (E_p) moves towards more negative potentials for EC and moves oppositely towards more positive potentials for CE mechanism, while peak currents (i_p) for both types of mechanisms decreases. As far as DV concerned, our recent work [31, 32] show that even slower electron transfer processes exhibits symmetry when electrode sphericity increases: this suggest that planar electrode is much more effective than the spherical electrode with the present DP method.

1.3.3 Similar analysis from differential pulse polarography (DPP)

Our group has adopted a different approach focusing on the analysis of *peak shapes in terms of symmetry parameters* as reported in our earlier studies on the first- and higher- order derivatives [12–15, 42], instead of examining shifts in peak potentials and changes in the magnitude of peak currents which is adopted by the other group [18, 54, 56]. Namely, in our previous studies [57–61], we have introduced the approach of analyzing peak asymmetry *found in the differential pulse polarography/voltammetry (DPP/DPV)* in terms of The differential pulse voltammograms can be viewed as a *pseudo-derivative of the i - E curve* which is emulated mechanically and/or electronically with the voltammetric/polarographic analyzer. In the earlier works, two peaks are generated from DPP; namely, a cathodic peak generated from a reduction process with a pulse going with the same direction as the scan direction (with a pulse amplitude of $\Delta E = -50$ mV), and an anodic peak generated with a pulse going against the scan direction (with $\Delta E = +50$ mV) to drive oxidation of reduced species back to the oxidized form, then the two peaks are compared and analyzed. In the original normal pulse program, the currents are assigned as positive for the reduction process. In the derivative voltammetry, however, if values of the derivative are positive or the peak appears in more positive potentials, it is labeled as “anodic”, if the values are negative, or the peak appears in more negative potentials, it is labeled as “cathodic” regardless of actual redox reaction occurring on the electrode surface, following the previous

convention [12–15, 42]. In addition to the analysis of peak in term of peak-currents and peak-potentials [57–60], an analysis in terms of half-peak-widths was introduced later [61]. In present study a focus is given more to the *second derivative* because (a) it generates two well-defined peaks of anodic and cathodic that parallel to two peaks of DPP, (b) it is more sensitive and practical than first derivative which has only one peak and fewer visible parameters, and (c) it is less complicated and more practical than third derivative even though it is less sensitive than the third derivative.

1.3.4 Other approaches for diagnostic criteria with cyclic square-wave voltammetry (CSWV)

Cyclic square-wave voltammetry (CSWV), which is an extension of SWV [62–65], has been adopted by Bottomley group [66–70]. Like pulse voltammetric techniques, SWV is effective in removing the interference from the capacitive current that is inherent in cyclic voltammetry (CV). SWV, like DPV, is a pseudo-derivative technique in which a derivative-shaped peak is obtained from the current with electronic control of input of square-wave potentials and current sampling times [62]. Diagnostic criteria as a tool for studying electrode mechanisms based on CSWV scheme have been investigated by the group for reversible [66] and quasi-reversible [67] processes, EC type [68], ECE type [69], CE type [70] mechanisms, and other non-unity stoichiometric cases [71]. Basically, the impact of experimental SW parameters - such as pulse heights (or amplitude), step heights (or potential increments), switching potentials, and period - on the peak-currents, peak-potentials and separations, peak-widths were examined. It was found that those observed peak-related quantities changes characteristically according to each particular types of the electrochemical mechanisms, which make it feasible to be utilized as diagnostic parameters.

2. Theory

2.1 Advantages of derivative approach

In general, original signals (y) from a measurement can be given in a polynomials of a dependent (x) variable:

$$y = ax^n + bx^{(n-1)} + cx^{(n-2)} + \dots + fx^2 + gx + h$$

Taking its firstst derivative of a signal above removes a constant component (h) which represent a background process yielding the signals, and taking 2nd derivative removes a linear component (gx term) which represent a secondary process for a signal component, thus revealing the hidden higher order processes. In other words, from these operations, (a) undesired components in the signal (a constant term, a linier component, and quadratic component) can be removed successively upon repeated differentiations) leaving higher order terms only. Thus, upon differentiations, changes (in- or de-creases) in the signal can be developed to yields peaks which were hidden behind the original signal; hence the better-defined peaks, makes the analysis of curve much easier than the original curves; thus revealing concealed features in the original function. Basically, higher order non-linear components in the function (original signals) transforms into peaks in the process of differentiations.

2.2 Peak currents, peak potentials, and peak widths and the ratios

Theoretical expressions for the first- second- and third- derivatives of current-potential curves were analytically derived from successive differentiations of the original current expression (i.e., zeroth order derivative) obtained; then the derivatives as function of potential were computed and plotted. The raw and derived parameters (**Figure 1**) for the simple reversible process (E_{rev}), calculated from the theoretical equations (Eq. 1–21; refer to Section 3.1.1) for lower order derivatives and those values given in the last column of **Table 1** -this analytical approach requires only a pencil and papers. However, for third derivatives for E_{rev} and all derivatives for other types (E_{irr} , CE_r , and E_rC), it is difficult to derive analytical solutions (equations) to calculate values of the parameter. Thus, numerical approaches had to be employed; namely, the values of a parameter as a function of an independent variable (such as a rate constant, k) had to be plotted on a graphs first, then a possible value or ranges of values were read from the graphs, and an equation for the relationships to calculate the parameters had to be found from such graphs, and this numerical approach requires much of computations, graph papers and a ruler. Those values of parameters, found analytically or numerically/ graphically are summarized (refer to the results sections for details) in **Table 2** for four types of the mechanisms for comparisons.

2.3 Obtaining theoretical derivatives for various types of electrode mechanisms - analytical method vs. numerical (digital) method

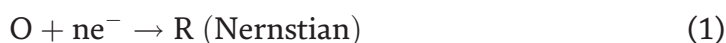
Theoretical equations of first, second and third for derivative for irreversible (and quasi reversible) processes are obtained with successive differentiations of analytical expressions of the current [15]. The derivatives of the CE type of mechanism are obtained with successive differentiations in a similar fashion [12, 13, 42]. Whenever possible, analytical solutions are sought after first because it is computationally less expensive. Numerical differentiations had to be adopted when analytical solution cannot be found. Thus, the analytical solutions of current expression and its first derivative for the EC type of mechanisms are so complicated that analytical differentiations for the second and third derivatives were practically impossible [11, 14], numerical differentiations had to be adopted [14]. A value of $\Delta E = 1.0$ mV was used for a finer resolution for all curves. The differentiation methods are summarized in **Table 3**.

3. Results and discussions

3.1 Derivation of the original current expression for various types of electrode mechanisms

3.1.1 Simple reversible electron transfer reaction (E_{rev} or E_r)

Theory Current (i) as a function of the applied potential (E), under semi-infinite linear diffusion, is expressed by the following relationship for a simple reversible electron-transfer process [1, 38]



$$i(E) = id [1/(1 + e)] \quad (2)$$

where

	Parameters	Definitions	E_r	E_{irr}	$E_r C$	CE_r	
Current	$E_{1/4}$ (mV)		+28	<28 (-205)			
	$E_{1/2}$ (mV)		0	<0 (-253)	>0	<0	
	$E_{3/4}$ (mV)		-28	<-28 (-295)			
	ΔE_q^a (mV)	$E_{1/4}-E_{1/2}$	28	>28 (48)	<28	>28	
	ΔE_q^c (mV)	$E_{1/2}-E_{3/4}$	28	>28 (42)	<28	>28	
	ΔE_h^0 (mV)	$E_{1/4}-E_{3/4}$	56.4	>56.4 (90)	<56.4	>51.5, <56.4	
	R_{qw}^0	$\Delta E_q^a/\Delta E_q^c$	1.0	>1.00 (1.14)	>1.00	<1.00	
	R_i^0 (normalized o E_r)		1.0	<1.0 (0.64)	1.0	<1.0	
1st Der.	ΔE_p^1 (mV)	E_p-E^0	0.0	<0.0 (-265)	>0	<0.0	
	i_p		9.6	<9.6 (6.4)	>9.6	<9.6	
	R_i^1 (normalized o E_r)		1.00	<1.00 (0.67)	>1.00	<1.00	
	$W_{1/2}$ (mV)		90.5	>90.5 (143)	<90.5	<90.5	
	W_q^a (mV)		45.3	>45.3 (80)	<45.3	>42, <45.3	
	W_q^c (mV)		45.3	>45.3 (63)	<45.3	>40, <45.3	
	R_w^1	W_q^a/W_q^c	1.00	>1.00 (1.27)	>1.00	<1.00	
	E_p^{2a} (mV)		34	<34 (-210)	<34	>34	
	E_p^{2c} (mV)		-34	<-34 (-319)	<-34	>-34	
	ΔE_p^2 (mV)	$E_p^{2a}-E_p^{2c}$	68	>68 (108)	<68	>59, <68	
	R_E^2	$\Delta E_p^{2a}/\Delta E_p^{2c}$	1.00	<1.0 (0.66)	>1.0	>1.0	
	i_p^{2a}		14	>14 (51)	>14	>10	
	i_p^{2c}		-14	<14 (-72)	>-14	>10	
	R_i^2	$ i_p^{2a}/i_p^{2c} $	1.00	<1.00 (0.71)	>0.71, <1.00	>1.0, <1.25	
	$W_{1/2}^{2a}$ (mV)		63	>63 (111)	>50, <63,	<63	
	$W_{1/2}^{2c}$ (mV)		63	>63 (81)	>35, <63	<63	
	R_w^2	$W_{1/2}^{2a}/W_{1/2}^{2c}$	1.00	>1.00 (1.37)	>1.00, <1.45	<1.0	
3rd Der.	E_p^{3a} (mV)		59	<59 (-165)	>59	>-180	
	E_p^{3m} (mV)		0.00	<0.00 (-275)	>0.00	>-230	
	E_p^{3c} (mV)		-59	<-59 (-353)	>-59	>-300	
	ΔE_p^3 (mV)	$E_p^{3a}-E_p^{3c}$	118	>118 (188)	<118	<118	
	ΔE_a^3 (mV)	$E_p^{3a}-E_p^{3m}$	59	>59 (110)	<59	<59	
	ΔE_c^3 (mV)	$E_p^{3m}-E_p^{3c}$	59	>59 (78)	<59	<59	
		$R_{\Delta E}^3$	$\Delta E^{3a}/\Delta E^{3c}$	1.00	>1.00 (1.41)	>1.0, <~1.6	<1.00
		i_p^{3a}		2461	<2461 (449)	<3692	<2461
		i_p^{3m}		-7382	>-7382 (-1961)	>-15500	>-7382
		i_p^{3c}		2461	<2461 (1061)	<8367	<2461
		R_i^3	i_p^{3a}/i_p^{3c}	1.00	<1.00 (0.42)	>0.4, <1.0	>1.0, <1.27
		R_i^{3a}	$ i_p^{3a}/i_p^{3m} $	0.32	<0.32 (0.22)	>0.2, <0.32	>0.32, <0.36
		R_i^{3c}	$ i_p^{3c}/i_p^{3m} $	0.32	>0.52 (0.52)	>0.32, <0.60	>0.28, <0.32
	$W_{1/2}^{3a}$ (mV)		54	>54 (102)	>50, <54	>42.5, <54	
	$W_{1/2}^{3m}$ (mV)		41	>41 (64)	>32, <54	>35, <41	

Parameters	Definitions	E_r	E_{irr}	E_rC	CE_r
$W_{1/2}^{3c}$ (mV)		54	>54 (63)	>32, <42	>50, <54
R_w^3	$W_{1/2}^{3a}/W_{1/2}^{3c}$	1.00	>1.00 (1.62)	>1.0, <1.7	>1.00, <1.19
R_w^{3a}	$W_{1/2}^{3a}/W_{1/2}^{3m}$	1.32	>1.32 (1.60)	>1.3, <1.6	>1.19, <1.32
R_w^{3c}	$W_{1/2}^{3c}/W_{1/2}^{3m}$	1.32	<1.32 (0.98)	>1.0, <1.3	>1.32, <1.43

Notes: (a) Calculated for $n=1$ and $T=298^\circ K$ for the reversible e^- transfer reaction (Third Column).

(b) All values for the irreversible case were calculated for $k^0=1.0 \times 10^{-5} \text{ cm/s}$ and $\alpha n=0.50$;

For the case with $\alpha n \neq 0.50$, these values are not restricted to the ranges given above. those values the parentheses are calculated with $k_s=1.0 \times 10^{-5} \text{ cm/s}$

(c) Values for quasi-reversible processes, calculated for $\alpha n=0.5$, lie in between those for reversible processes and those for irreversible processes, hence the column for quasi-reversible cases is omitted.

Table 2.

Comparisons of values independent variable and derived parameters for various mechanisms.

Types of Mechanisms	Current i	1 st Der. i'	2nd Der. i''	3rd Der. i'''
		di'/dE	di''/dE	di'''/dE
$E_r(\text{rev})$	i	di'/dE	di''/dE	di'''/dE
$E_{irr}(\text{irreversible})$	i	di'/dE	di''/dE	di'''/dE
CE_r (Prior Chemical)	i	di'/dE	di''/dE	di'''/dE
E_rC (Post Chemical)	i	di'/dE	$\Delta i''/\Delta E$ (numerical)	$\Delta i'''/\Delta E$ (numerical)

Table 3.

Methods of differentiation for various electrode mechanisms. Derivatives are obtained from the analytical solutions of currents for each cases, except for i'' , i''' with the post kinetics system (E_rC).

$$i_d = nFAD_0^{1/2}C_0/(\pi t)^{1/2} \text{ (the diffusion – controlled current)} \quad (3)$$

$$e = \exp(nFE/RT) \quad (4)$$

and E is an applied potential with respect to the reversible polarographic half-wave-potential, $E_{1/2}(\text{rev})$ or E_h . Other parameters and variables have their usual meanings. Eq. 2 is derived assuming $D_O = D_R$. Successive differentiations of Eq. 2 with respect to E yields [15].

$$i'(E) = -i_d(nF/RT) \left[e/(1+e)^2 \right] \quad (5)$$

$$i''(E) = -id(nF/RT)^2 \left[e(e-1)/(1+e)^3 \right] \quad (6)$$

$$i'''(E) = -id(nF/RT)^3 \left[e(e^2 - 4e + 1)/(1+e)^4 \right] \quad (7)$$

Examination of Eq. 2 reveals that

$$i(-E) = i_d - i(E) \quad (8)$$

$$i(0) = i_d/2 \quad (9)$$

This implies that the i - E curve (solid line, **Figure 1A**) is symmetrical with respect to its inflection point $(0, i_d/2)$.

3.1.1.1 For the first derivatives

Eq. 5 shows

$$i'(-E) = i'(E) \quad (10)$$

This means that the *first derivative is symmetrical with respect to an axis $E = 0$* (**Figure 1B**, solid line). The value of the peak-width at a half-height for the reversible process proved to be 90.5/n mV at 298 K [18]. A shape parameter from the first derivative can be defined; the peak widths are divided into positive (anodic) and negative (cathodic) parts to define two semi-peak widths (W_q^a and W_q^c , **Figure 1B**) and their ratios. For a reversible process it was found [14].

$$W_{1/2} = 90.5 \text{ mV} \quad (11)$$

$$W_q^a = W_q^c = (1/2)W_{1/2} = 45.3/n \text{ mV at } 298 \text{ K} \quad (12)$$

$$W_q^a/W_q^c = 1 \text{ at any temperature} \quad (13)$$

3.1.1.2 For the second derivatives

One can examine the second derivative (i''), Eq. (6), to find

$$i''(-E) = -i''(E) \text{ and } i''(0) = 0 \quad (14)$$

Thus, the second derivative (**Figure 1C**, solid line) *has the same symmetry as the current with respect to its inflection point*. One can define shape parameters $W_{1/2}^{2a}$ and $W_{1/2}^{2c}$ which are the peak-widths for the anodic (positive) and cathodic (negative) peaks in the second derivative. It should be pointed out that the adjectives “anodic” and “cathodic” in this context are *not* related to the actual redox processes associated with the peaks. The two peak heights for the anodic, i_p^{2a} , and the cathodic, i_p^{2c} , peaks are defined at two peak potentials, E_p^{2a} and E_p^{2c} , respectively (**Figure 1C**).

Following relationships are found for E_r type.

1. Peak Potentials

$$E_p^{2a} - E_p^{2c} = 68/n \text{ mV (at } 298 \text{ K)} \quad (15)$$

$$|E_p^{2a}/E_p^{2c}| = 1.00 \quad (16)$$

2. Peak Currents

$$i_p^{2a} = -i_p^{2c} \quad (17)$$

$$|i_p^{2a}/i_p^{2c}| = 1.00 \quad (18)$$

3. Peak Widths

$$W_{1/2}^{2a} = W_{1/2}^{2c} = 62.5/n \text{ mV (at } 298 \text{ K)} \text{ or} \quad (19)$$

$$W_{1/2}^{2a}/W_{1/2}^{2c} = 1.00 \quad (20)$$

The peak-potentials in Eq. 15 can be found by solving $i''(E) = 0$ (Eq. 7) for E .

$$-id(nF/RT)^3 \left[e(e^2 - 4e + 1)/(1 + e)^4 \right] = 0 \quad (21)$$

As given in the value of the unity (1.0) for those symmetry parameters (i.e. anodic to cathodic peak-current ratios, anodic to cathodic half-peak-width ratios, and anodic to cathodic peak potential ratios) for first or second derivatives, the derivatives are curves are symmetrical.

3.1.1.3 For the third derivatives

It's symmetry is the same as that of the first derivative, *being symmetrical with respect to $E = 0$* . One can find the ranges of parameter values in similar fashion for the third derivatives. Details of the work can be found elsewhere [15]: the key findings on the peak potentials, peak current and half peak widths and the various ratio for symmetry are given in **Tables 1** and **2**. It should be noted that all those values for the anodic to cathodic symmetry parameters (Q 's) are unity, the same as in lower order derivatives.

As shown above, the values of parameters above for E_r process are derived analytically from the equations which are much simpler than others. However, for an irreversible electron process (E_{irr} , or $E_{quasirev}$) and chemically coupled electron transfer reactions such as E_rC and CE_r , the expressions for the current and their derivatives are so complicated that it is impossible to derive the values of those parameters analytically by solving algebraic equation (Refer to later section). Therefore, a numerical approach had to be adopted. Namely, (a) about 10 curves for derivatives vs. potentials at various values of independent variables (the heterogeneous rate constant k^o and αn for simple electron e^- transfer; the homogeneous constant K_{eq} , k_f , k_b and k for chemically coupled electron transfer) had to be calculated, (b) then, all those curves are plotted out, and (c) those plots are analyzed graphically by examining the curves carefully in order to obtain values or equations (relationships) for those parameters.

3.1.1.4 Simple values of symmetry parameters of reversible electrochemical process (E_r)

The symmetric relationship among the symmetry parameters are found from the simple fast electron transfer process; namely, a reversible electron transfer (E_{rev} , or E_r) type in which the electrode process is basically Nernstian. What will happen to the shapes of voltammograms and its derivatives if the system involve non-Nernstian behavior with a slower irreversible electron transfer rate (E_{irr} type), or the electron transfer is coupled with a prior chemical equilibrium (CE_r Type) or an E_r coupled with a follow-up chemical reactions (E_rC). These studies have been already done mostly and discussed in detail by our group [14]; to summarize, the symmetry exhibited in the derivatives in E_r disappears for the non-Nernstian electron transfer (i.e., irreversible) system. Namely, the asymmetry strongly depends on those the electron transfer parameters (α and k^o) for E_{irr} type, and the kinetic parameters (i.e., k and K_{eq}) for chemically coupled processes (C_rE_r and E_rC_{irr} Type). In this work, comparisons are made for the symmetry parameters for the different electrode mechanisms. Details are given in later sections for each of corresponding mechanisms.

3.1.1.5 Reversibility in electrochemical reactions

In general, reversibility in electrochemical reactions is divided into three kinds depending on the magnitude of the standard heterogeneous rate constant k^o (or k_s)

with respect to the diffusion coefficient (D): an electron transfer reaction is considered reversible if e-transfer is much faster the diffusion (i.e., $k^o \gg (D/t)^{1/2}$), and irreversible if e-transfer is much slower the diffusion ($k^o \ll (D/t)^{1/2}$) and quasi-reversible if those competing rates are comparable ($k^o \sim (D/t)^{1/2}$).

In terms of values of k^o , by adopting typical values of D ($=5 \times 10^{-5} \text{ cm}^2/\text{s}$) and t ($=1.000 \text{ s}$).

reversible for $k^o > 0.020 \text{ cm/s}$,

quasi-reversible for $0.020 \text{ cm/s} > k^o > 5 \times 10^{-5} \text{ cm/s}$, and.

irreversible for $k^o < 5 \times 10^{-5} \text{ cm/s}$.

In the following sections, other types of processes than the simple reversible process will be treated.

3.1.2 Theoretical expression for and the derivatives for $E_{quasirev}$ and E_{irr} types of electron transfer

Currents (i) as a function of the applied potential (E) for non-Nernstian (i.e., irreversible and quasi-reversible) system with a slower electron transfer, have been previously derived and given in several references [44, 54–56, 72, 73], and has final forms of the following equations for a planar diffusion:

$$I = nFAC_0k_f [\exp(Q^2t)\text{erfc}(Qt^{1/2})] \quad (22)$$

assumed $D_R = D_O = D$.

All symbols have their usual meanings and may be refer to the reference for details,

where,

$$Q = (k_f + k_b)/D^{1/2} \quad (23)$$

$$k_f = k^o \exp \{-\alpha nF(E - E^o)/RT\} \quad (24)$$

$$k_b = k^o \exp \{(1 - \alpha)nF(E - E^o)/RT\} \quad (25)$$

$$E_{1/2} = E^o + (RT/nF) \ln (D_R/D_O)^{1/2} = E^o \quad (26)$$

normalizing the current, Eq. (22), to the diffusion current, Eq. (3), yields

$$i_n = (\pi t/D)^{1/2} k_f [\exp(Q^2t)\text{erfc}(Qt^{1/2})] \quad (27)$$

where,

$$F(Qt^{1/2}) = \exp(Q^2t)\text{erfc}(Qt^{1/2}) \quad (28)$$

This normalized current, which is independent of the concentration and electrode surface area, mostly is dependent on the heterogeneous rate constants (k^o), the transfer coefficient (α) and n, and the curve found to exhibit an asymmetry [15].

Successive differentiations of the current yield the following expressions for the first-, second- and third- derivatives respectively [15]. Taking derivative of the current with respect to potential (E) yield the first derivative,

$$i' = (\pi t/D)^{1/2} k_f \left[(-nF/RT)F(Qt^{1/2}) + 2Q' \left[QtF(Qt^{1/2}) - (t/\pi)^{1/2} \right] \right] \quad (29)$$

where

$$Q' = (-\alpha nF/RT)k_f/D_o^{1/2} - ((1 - \alpha)nF/RT)k_b/D_r^{1/2} \quad (30)$$

The analytical differentiations of i' and expressions for the second- and third-derivatives are more involved and given elsewhere [15]. Alternatively, it is also possible to obtain second and third derivative curves from successive *numerical* differentiations starting from the values of first derivative.

As shown above, the current expression for or an irreversible e^- transfer and quasi-reversible much complicated than that of reversible case, because the current depends not only on the applied potential but also k^o and αn which introduces much differences in the peak shapes and peak symmetry. Comparisons of the cases are made in **Figure 2** for a contrast for E_r and E_{irr} processes.

It can be readily seen from the curves that as the reduction becomes more difficult (i.e., with smaller k^o) (a) all curves shifts to negative (cathodic) direction for the quasi-reversible and irreversible process, (b) the curves and peaks become widened, and (c) the curve becomes asymmetric which is much pronounced in the second and third derivatives although it is not readily seen from the current and its first derivative. By analyzing the formula and the curves graphically, one can find possible values and their ranges for the following variables or asymmetric parameters listed on **Table 1**: such values of the irreversible process are summarized in **Table 2** along with those of the reversible process for comparisons.

3.1.2.1 For the first derivative

First derivative is obtained by differentiating Eq. (27) and (28), the details of differentiation and the results were given elsewhere in original work [15] of the author's group: for the irreversible or quasi-reversible process, following relationships are found from plots

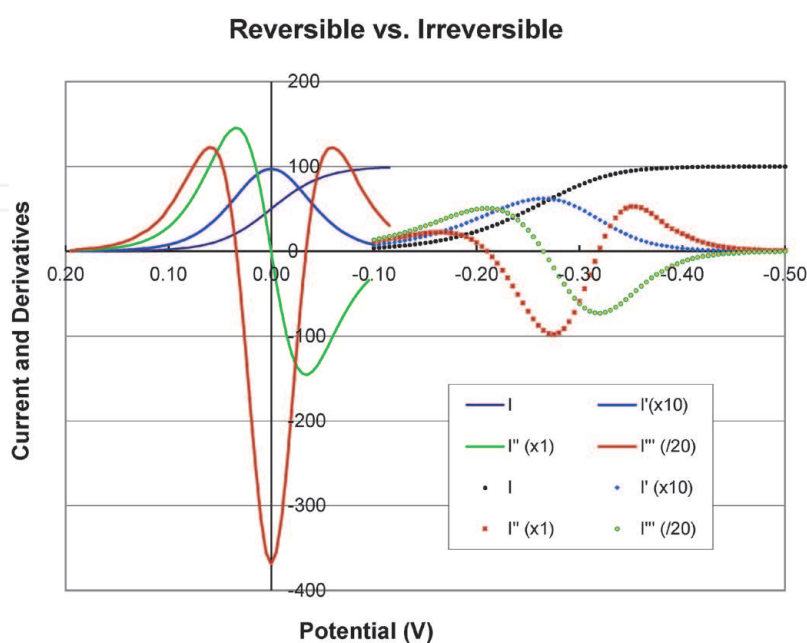


Figure 2.

Comparison of currents (normalized at 100, black), and their first (blue), second (green), and third derivatives (red). Those for a simple reversible electron transfer are given in solid lines on the left, and those for an irreversible electron transfer reaction (with $k^o = 10^{-5}$ cm/s, $n = 1$, and $\alpha = 0.5$ at $T = 298$ K) are in dotted lines on the right. The derivatives were scaled appropriately in order to bring all of them in the same plotting area: Scaling factors are given in the parentheses.

1. Peak Potentials

It is found that the peak potential for totally irreversible process ($k^{\circ} < 10^{-5}$ cm/s) is directly proportional to $\log(k^{\circ})$, shifting towards cathodic direction as k° decreases for a given αn , and is inversely proportional to αn at a constant k° [15].

$$E_p = E^{\circ} + [(60.3) \log(k^{\circ}) + 165](1/\alpha n) \text{ (mV)} \quad (31)$$

< 0 (because $\log(k^{\circ})$ is always negative for E_{irr}).

2. Peak Currents

The normalized peak heights is directly proportional to αn , decreasing from 9.6 (for E_r) to 6.2 as k° decreases [15]

$$i_p/i_d = 12.3(\alpha n) \sim 6.2 < 9.6 \text{ for } \alpha n = 0.5 \quad (32)$$

3. Peak-Widths.

The half-peak width ($W_{1/2}$), the anodic half-peak width (W_q^a), and the cathodic half-peak width (W_q^c) at 298 K for a totally irreversible reaction are independent of k° , but inversely proportional to αn [15]

$$\begin{aligned} W_{1/2} &= 2.80(RT/F)(1/\alpha n)(V) = 72(1/\alpha n)(mV) \\ &= 144 \text{ (mV)} > 90.4 \text{ (mV)} \quad \text{for } \alpha n = 0.5 \end{aligned} \quad (33)$$

$$\begin{aligned} W_q^a &= 1.62(RT/F)(1/\alpha n)(V) = 41.7(1/\alpha n)(mV) \\ &= 83.4 \text{ (mV)} > 45.3(mV) \text{ for } \alpha n = 0.5 \end{aligned} \quad (34)$$

$$\begin{aligned} W_q^c &= 1.26(RT/F)(1/\alpha n)(V) = 32,4(1/\alpha n)(mV) \\ &= 64.8 \text{ (mV)} > 45.3(mV) \text{ for } \alpha n = 0.5 \end{aligned} \quad (35)$$

$$W_q^a/W_q^c = 1.28 > 1.00 \text{ for all } \alpha n \quad (36)$$

3.1.2.2 For the second derivative

Second derivative was obtained by differentiating the first derivative, Eq. (8) and (29) The details of the derivation and the results are given elsewhere and following relationships were found [15]:

1. Peak-Potentials and Peak Separation

Both peak potentials (anodic and cathodic) of the second derivatives for totally irreversible processes ($k^{\circ} < 10^{-5}$ cm/s) are directly proportional to $\log(k^{\circ})$ for a given αn , moving to cathodic direction as k° decreases, which is the same trend as for E_p in the first derivative.

$$E_p^{2a} = E^{\circ} + \{(60.3) \log(k^{\circ}) + 201\}(1/\alpha n) \text{ (mV)} \quad (37)$$

$$E_p^{2c} = E^{\circ} + \{(60.3) \log(k^{\circ}) + 67\}(1/\alpha n) \text{ (mV)} \quad (38)$$

$$\begin{aligned} \text{and } E_p^{2a} - E_p^{2c} &= 2.3(RT/F)(1/\alpha n) = 0.0591(1/\alpha n) \text{ (mV)} \\ &= 118 \text{ mV} > 68mV \text{ for } \alpha n = 0.5 \end{aligned} \quad (39)$$

Both peak potentials (E_p^{2a} and E_p^{2c}) are dependent on k^o as well as αn values yielding -210 mV and -319 mV respectively, with $k^o = 10^{-5}$ cm/s and $\alpha n = 0.5$. However, the peak potential difference depends only on αn values, not on k^o .

$$\Delta E_p^{2a} / \Delta E_p^{2c} = 210\text{mV} / 319\text{mV} = 0.66 < 1.00 \quad (40)$$

2. Peak-Heights and Their Ratios.

A plot of the two peak-heights (i_p^a for anodic and i_p^c cathodic side) of the second derivative depend heavily on αn , a magnitude of both heights increases with increasing αn . However, i_p^c is greater than i_p^a for most of the case unless $\alpha n = 0.3$ which is strange.

$$|i_p^a / i_p^c| = 0.78 < 1.00 \text{ for } \alpha n = 0.5 \quad (41)$$

3. Peak-Widths and Their Ratio.

Two half-peak-width (anodic and cathodic) of the second derivatives, and the ratio for E_{irr} processes are given below

$$\begin{aligned} W_{1/2}^{2a} &= 2.10(RT/F)(1/\alpha n) \text{ (V)} = 54.0(1/\alpha n) \text{ (mV)} \\ &= 108 \text{ mV} > 64 \text{ mV for } \alpha n = 0.5 \end{aligned} \quad (42)$$

$$\begin{aligned} W_{1/2}^{2c} &= 1.53(RT/F)(1/\alpha n) \text{ (V)} = 39.4(1/\alpha n) \text{ (mV)} \\ &= 78.8 \text{ mV} > 64 \text{ mV for } \alpha n = 0.5 \end{aligned} \quad (43)$$

$$W_{1/2}^{2a} / W_{1/2}^{2c} = 1.37 > 1.00 \text{ for all } \alpha n \quad (44)$$

Here again, it should be noted that although the two half-peak-widths depends on αn , their ratio is invariant.

3.1.2.3 For the third derivatives

Third derivative are obtained by differentiating the second derivative. The details of the derivation and results were given elsewhere [15]. The number of parameters increases, and results on the parameters increase as three peaks are available, and those parameters (peak separations, peak-current ratios, and half-peak ratios. Were analyzed from various plots. The results with possible ranges of the values are summarized in **Table 2**.

3.1.2.4 Sensiivity increases with increasing order of derivatives

In **Table 2**, the key results from irreversible process (as well as two chemically coupled process) are juxtaposed here for a ready comparison of the differences observed among the types of mechanisms. Basically, the symmetry observed in the curves for the reversible process, disappears as the electron transfer rates become slower (i.e., irreversible type): the unity (1.00) values of the ratio parameters becomes no longer 1.00 for irreversible (E_{irr}) process and for other types of electrode mechanisms. Namely, the ratio of anodic to cathodic peak-widths ($W_{1/2}^a / W_{1/2}^c$) increases to 1.27 (an increase of 27%) for the first derivative, and it increases to 1.37 (an increase of 37%) for the second derivative, while it increases to 1.62 (an increase of 62%) for the third derivative. In general these ratios increases systematically, as an order of a derivative increases; the higher the order is, the larger the changes are.

These changes (or sensitivity) of symmetry parameter values with increasing order of a derivative are also observed in CE_r as well as E_rC . In short, the values of the symmetry parameters with a ratio of anodic values to cathodic values (all R 's) are 1.00 for reversible electron transfer reactions; however it will deviates from the unity (<1.00 or >1.00) for other types of processes as shown in later sections.

3.1.2.5 Notes on computations for quasi-reversible and irreversible processes

All computations are carried out with $k^o = 1.0 \times 10^1$ cm/s for a reversible case, $k^o = 1.0 \times 10^{-3}$ cm/s for a quasi-reversible case, $k^o = 1.0 \times 10^{-5}$ cm/s for an irreversible case for simple e^- transfer reactions. A value of αn of 0.50 is used for all quasi-reversible and irreversible cases. For quasi-reversible processes, only the case with $\alpha n = 0.5$ is reported. The values for all parameters for quasi-reversible process (with $\alpha n = 0.5$) lies in between those for reversible and those for irreversible case. Those values for quasi-reversible case with $\alpha n \neq 0.5$ exhibits much complicated behaviors depending on values of αn [15]. This is because depending on values of the kinetic parameters (k^o and αn) the changes in some dependent variables become not monotonic, often exhibiting discontinuity at around $\alpha n = 0.3$.

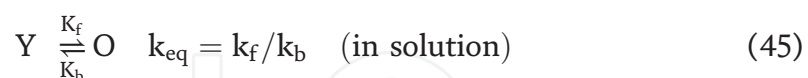
Propagations of round-off errors, associated with differentiations (or subtractions) which result in a loss of significant figures, encountered in evaluating the derivatives (Eq. 27–30): the error were so severe that an extended quadruple-precision mode (32 significant digits) had to be employed for all calculation: namely, the function $\exp(x^2)\text{erfc}(x)$: namely $F(Q_s t^{1/2}) = \exp(Q_s^2 t)\text{erfc}(Q_s t^{1/2})$ (Eq. 28) had to be evaluated to the 32 digit-precision [13].

3.1.3 Reversible electron transfer coupled with a prior chemical equilibrium (CE_r)

3.1.3.1 Theoretical expressions for and the derivatives

Full derivations of the derivatives from a current expression are given elsewhere [1, 12, 13]: the basic reaction scheme and final forms of formula are presented here.

This mechanism that involves pre-chemical step can be given as follows.



At a more interesting case of $K_{eq} \ll 1$, the currents [1, 13] is given by

$$i = i_d \left[(\pi t)^{1/2} (K_{eq} k_f)^{1/2} \exp(K_{eq} k_f (1 + e)/K_{eq})^2 t \right] \text{erfc} \left((K_{eq} k_f)^{1/2} (1 + e)/K_{eq} t^{1/2} \right) \quad (47)$$

Successive differentiations of the current yield the first-, second- and third-derivatives, respectively.

$$i' = i_d (nF/RT) (2k_f t) e \left[(1 + e/K_{eq}) i - 1 \right] \quad (48)$$

Second derivative becomes

$$i'' = i_d (nF/RT)^2 (2k_f t) e \left[(1 + e/K_{eq}) i + (RT/nF) (1 + e/K_{eq}) i' - 1 \right] \quad (49)$$

Third derivative becomes

$$i''' = i_d(nF/RT)^3(2k_f t)e \left[(1 + 4e/K_{eq})i + (2RT/nF)(1 + 2e/K_{eq})i' + (RT/nF)^2(1 + e/K_{eq})i'' - 1 \right] \quad (50)$$

Such curves according to the derivative formula are given in **Figure 3**. Full details of derivations of the three derivatives above and the analysis of the all parameters from those graphs were presented elsewhere [12, 15, 42], and only important key results are presented here, and summarized in the **Tables 2 and 4**.

Typical i - E curves at various k_f value for CE process are given **Figure 3A** in two dimensions, and **Figure 4A** in three dimensions with an additional axis for $\log(k_f)$. The plots of the original currents and three derivatives were calculated according to the Eq. (47), (48), (49), and (50). As it can be expected the entire i - E curve moves upward with the diffusion-controlled current as k_f increases. Asymmetry is not readily noticeable in the current and first derivatives, but it becomes more visible in the second and third derivatives: namely, anodic side of the peak height is larger than the cathodic side in both second and the third derivatives, This is more evident for larger k_f where currents are larger in all potentials. All the relationships are obtained graphically [12, 42], because finding the analytical solution of the dependent variables and parameters from the theoretical equations are too involved to be calculated. Graphic analysis of the curves yields the following results: the full account for the analysis of the derivative curves can be found in Ref. [12, 42].

3.1.3.2 For the first derivative

For a CE_r process, following relationships can be obtained from analysis of the graphs for the first derivative.

1. Peak-Potentials

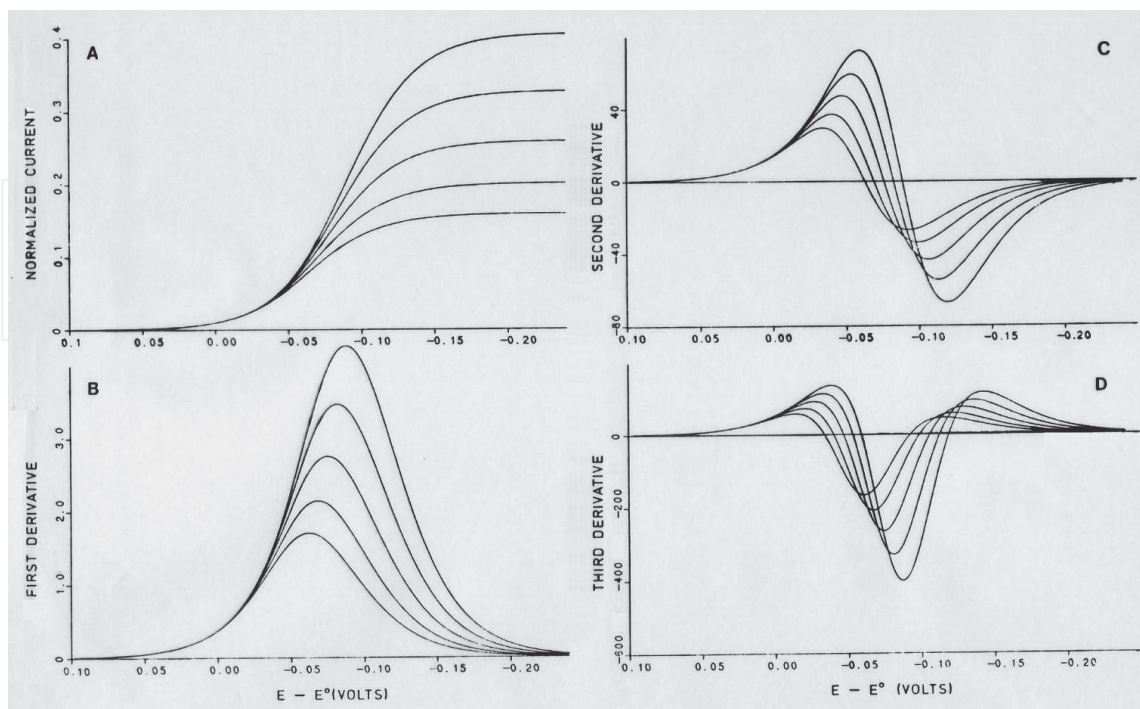


Figure 3. Normalized currents (a), their first (B), second (C) and third (D) derivatives at various values of forward rate constant at $K_{eq} = 10^{-2}$ for CE_r type mechanism: (a) $k_f = 10 \text{ s}^{-1}$ (for the lowest current and derivatives), (b) 5.62, (c) 3.16, (d) 1.78, (e) 1.00 (for the highest current and derivatives), calculated for $T = 298$, $t = 1.0$, and $n = 1$.

Parameters	Definitions	E_r	E_{irr}	E_rC	CE_r
Current					
ΔE_h^0 (mV)	$E_{1/4} - E_{3/4}$	56.4	>56.4 (90)	<56.4	>51.5, <56.4
R_q^0	$\Delta E_q^a / \Delta E_q^c$	1.00	>1.00 (1.14)	>1.00	<1.00
1st Der.					
$W_{1/2}$ (mV)	90.5	>90.5 (143)	<90.5	>90.5	
R_w^1	W_q^a / W_q^c	1.00	>1.00 (1.27)	>1.00	<1.00
2nd Der.					
ΔE_p^2 (mV)	$E_p^{2a} - E_p^{2c}$	68	>68 (108)	<68	>59, <68
$R_{\Delta E}^2$	$\Delta E_p^{2a} / \Delta E_p^{2c}$	1.00	<1.0 (0.66)	>1.00	>1.00
R_i^2	$ i_p^{2a} / i_p^{2c} $	1.00	<1.00 (0.71)	>0.71, <1.00	>1.0, <1.25
R_w^2	$W_{1/2}^{2a} / W_{1/2}^{2c}$	1.00	>1.00 (1.37)	>1.00, <1.45	<1.00
3rd Der.					
$R_{\Delta E}^3$	$\Delta E^{3a} / \Delta E^{3c}$	1.00	>1.00 (1.41)	>1.0, <~1.6	<1.00
R_i^3	i_p^{3a} / i_p^{3c}	1.00	<1.00 (0.42)	>0.4, <1.0	>1.0, <1.27
R_i^{3a}	$ i_p^{3a} / i_p^{3m} $	0.32	<0.32 (0.22)	>0.2, <0.32	>0.32, <0.36
R_i^{3c}	$ i_p^{3c} / i_p^{3m} $	0.32	>0.52 (0.52)	>0.32, <0.60	>0.28, <0.32
R_w^3	$W_{1/2}^{3a} / W_{1/2}^{3c}$	1.00	>1.00 (1.62)	>1.0, <1.7	>1.00, <1.19
R_w^{3a}	$W_{1/2}^{3a} / W_{1/2}^{3m}$	1.31	>1.31 (1.60)	>1.31, <1.6	>1.19, <1.31
R_w^{3c}	$W_{1/2}^{3c} / W_{1/2}^{3m}$	1.31	<1.31 (0.98)	>1.0, <1.31	>1.31, <1.43

Notes: All values calculated with the same conditions as in Table 2.

Table 4.

Summary of asymmetry parameters which are more sensitive to the kinetics.

Peak potentials always shifts to more cathodic direction as the equilibrium constant for the prior chemical step, K_{eq} (or k_f), becomes smaller. Namely, E_p is more negative than E^0 ,

$$E_o - E_p > 0.0 \quad (51)$$

2. Peak Current

Normalized peak currents found to be smaller than 9.6.

As expected, i_p decreases as K (hence k_f) decreases from the reversible value of 9.6

$$i_p < 9.6 \quad (52)$$

3. Peak Width

Half-peak-widths become less than $90.4/n$ (mV), approaching to $80/n$ mV as K (hence k_f) decreases

$$W_{1/2} < 90.5/n \text{ (mV)} \quad (53)$$

The anodic part of a half-peak is always smaller than the cathodic part.

$$W_q^a < W_q^c < W_q^a \text{ (rev)} < W_q^c \text{ (rev)} = 90.5/n \text{ (mV)} \quad (54)$$

$$W_q^a / W_q^c < 1.00.$$

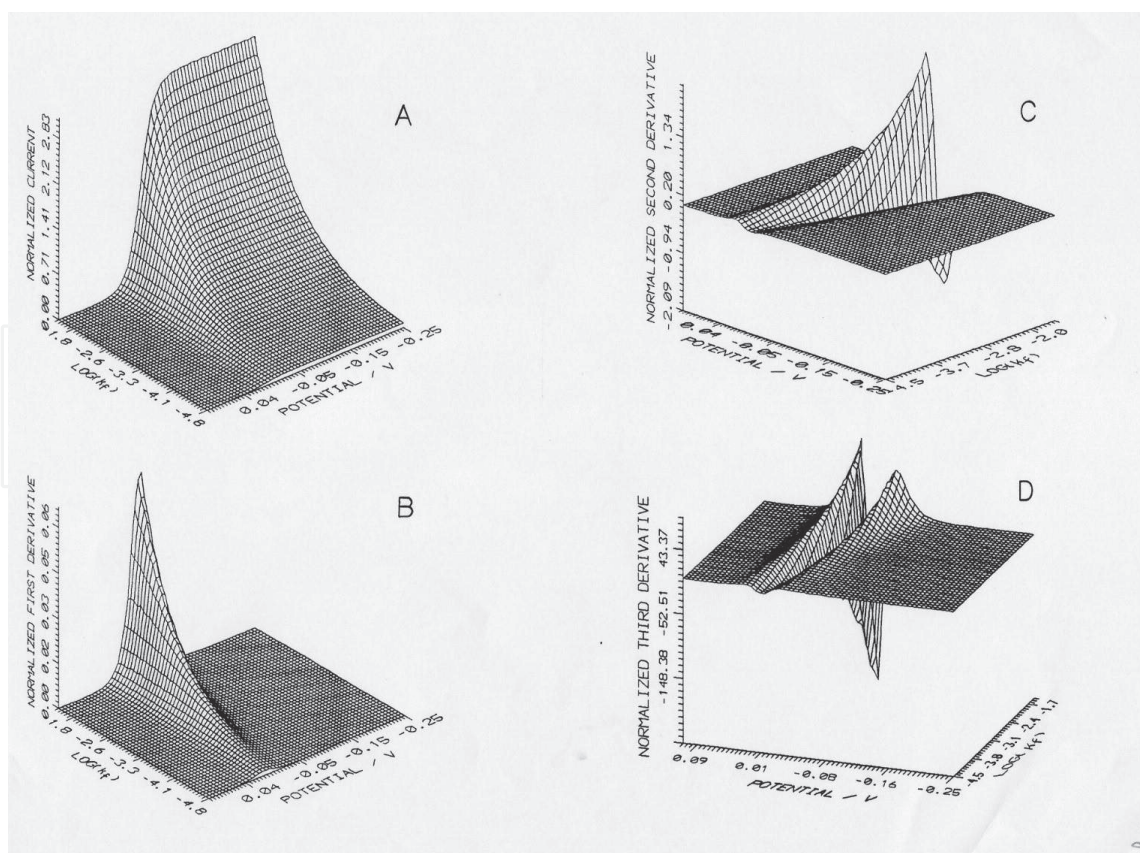


Figure 4.

Three-dimensional plots of normalized current-potential (i - E) curves at various forward rate constants (k_f) with $K_{eq} = 10^{-4}$. The perspectives of the current (A) and first derivative (B) is different from those of the second (C) and third derivatives (D) for a better view of valleys present in second and third derivatives.

3.1.3.3 For the second derivative

Following relationships can be obtained from analysis of the graphs for the second derivative.

1. Peak-Potentials and Peak Separation and the Ratio

The separation of the two peaks decreases as K (hence k_f) from $68.0/n$ (mV), the value for E_r .

$$E_p^{2a} - E_p^{2c} < 68.0/n \text{ (mV)}$$

$$\Delta E_p^{2a} / \Delta E_p^{2c} > 1 \quad (55)$$

2. Peak Currents and the Ratio

It is observed that the anodic peak currents are always larger than the cathodic ones, but smaller than 1.25.

$$i_p^{2a} / i_p^{2c} > 1.00 \quad (56)$$

3. Peak Widths and the Ratio

The anodic half-peak is always smaller than the cathodic one

$$W_{1/2}^a < W_{1/2}^c < W_{1/2}^a \text{ (rev)} < W_{1/2}^c \text{ (rev)} = 64/n \text{ (mV)} \quad (57)$$

$$W_q^a / W_q^c < 1.00$$

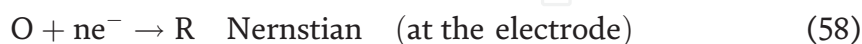
3.1.3.4 For the third derivative

Parameters associated with the third derivatives can be graphically analyzed in a similar fashion, and the results are given in the **Table 2** for the various values for three peaks, peak separations, peak-current ratios, and half-peak ratios. Refer to Ref. 12, 42 for full details.

3.1.4 Reversible Electron transfer coupled with a follow-up chemical reaction (E_rC)

3.1.4.1 The mechanism and derivation of the current and its derivatives

This e^- transfer reaction with a post kinetic process mechanism can be given as follows [11].



The closed form of the analytical solution of the concentration gradient and the current at the specific of the boundary conditions for this E_rC mechanism can be found elsewhere, but the solutions for the current include Dawson Integrals are too lengthy and complicated to be reproduced here and can be found elsewhere [11]. Nonetheless, we managed to obtain the first derivatives by analytically differentiating the current equation. However, further analytical differentiation of the first derivative in order to obtain second and third derivatives were nearly impossible; thus, a numerical approach had to be adopted; namely, the two higher order derivatives i.e., (second and third derivatives) were obtained with ΔE being as small as 1 mV in order to increase a resolution of peaks [14]. Such derivatives thus obtained are given in **Figure 5**. In general, all curves shift to the left anodic direction as the rate constant (k) increases.

3.1.4.2 For the first derivative

For an E_rC type of mechanisms, following relationships have been observed from the analysis for the first derivative.

1. Peak Potentials

Peak potentials always shifts to anodic direction as the rate constant (k) for the follow up chemical reaction increases. Namely, E_p is more positive than E° ,

$$E_o - E_p < 0.0 \quad (60)$$

2. Peak Currents

Peak currents increase from 9.6 (the value for E_r) as the rate constant (k) increases, a current value of 12.3 was found, thus

$$i_p > 9.6 \quad (61)$$

i_p (normalized) > 1.00.
 which is opposite of CE_r .

3. Peak Width

Half peak-width is decreases from $90.5/n$ (mV) as the rate constant (k) increases,

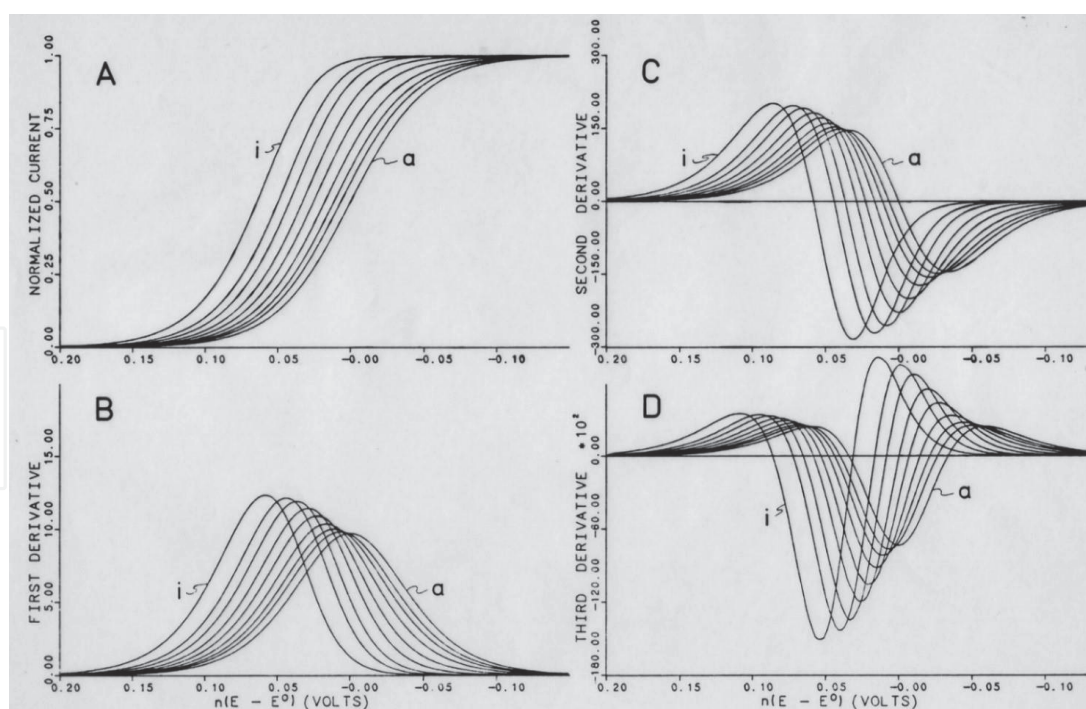


Figure 5.

Theoretical normalized current (A), and its first (B), second (C), and third derivatives (D) at various values of the homogeneous rate constant (k) for the E_rC type of electrode reaction. Calculated for k values of (a) 0 (b) 0.3, (c) 0.562, (d) 1.0, (e) 1.78, (f) 3.0, (g) 5.62, (h) 10.0 (i) 30.0 s^{-1} , and $T = 298 \text{ K}$ and $t = 0.952 \text{ s}$. The normalized currents are dimensionless; thus, the first derivatives are in a unit of V^{-1} , second derivatives in V^{-2} , third derivatives in V^{-3} .

$$W_{1/2} < 90.5 \text{ (mV)} \quad (62)$$

The anodic part of a half-peak is always larger than the cathodic part.

$$W_q^c < W_q^a < W_q^a(\text{rev}) = W_q^c(\text{rev}) = 45.3/n \text{ (mV)} \quad (63)$$

$$W_q^a/W_q^c > 1.00 \quad (64)$$

It should be noted again that these trends are the opposite of those from CE_r type.

3.1.4.3 For the second derivative

Following relationships have been observed from the analysis of the second derivative.

1. Peak-Potentials and Peak Separation

As shown in **Figure 6**, both peak potentials shift anodically, and the separations of the two peaks decrease from 68.0n (mV) and approach to 54 mV as the rate constant (k) increases.

$$54/n \text{ (mV)} < E_p^{2a} - E_p^{2c} < 68.0/n \text{ (mV)} \quad (65)$$

This suggests that the homogeneous rate constant, k , can be directly determined from the measurements of the peak separation of the second derivative.

2. Peak-Currents and their Ratio

As shown in **Figure 7**, normalized values of both peak currents increase with increasing k . However, the peak current ratios always decrease from 1.0 to about 0.71 as k increases.

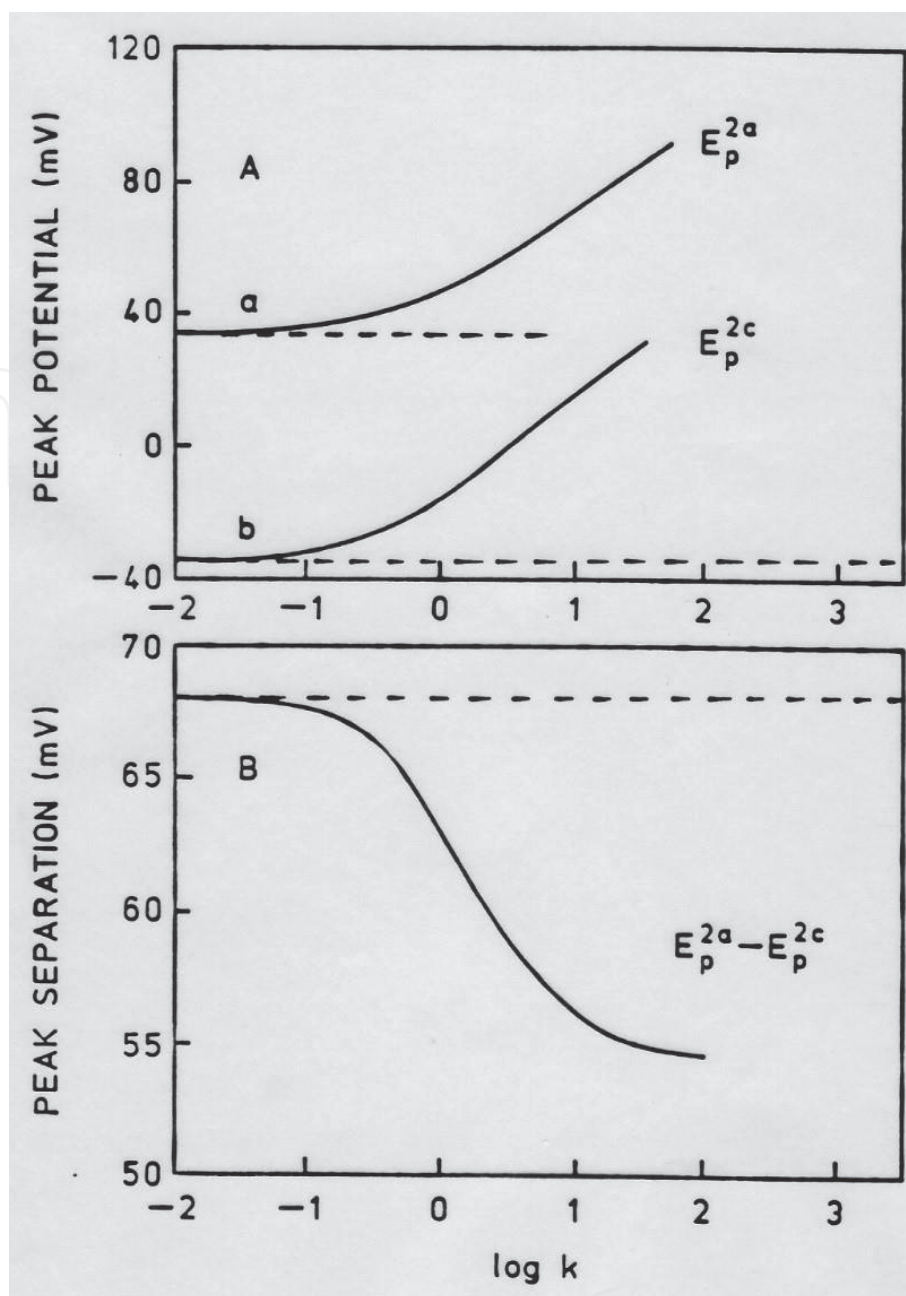


Figure 6. Effect of k (A) on the (a) the anodic, (b) cathodic peak potentials of the second derivative, (B) effect of k on the peak separation ($E_p^{2a} - E_p^{2c}$).

$$0.71 < |i_p^{2a}/i_p^{2c}| < 1.00 \quad (66)$$

This implies that the rate constant, k , can be directly determined from the measurements of the peak currents ratio of the second derivatives.

3. Peak-Widths and their Ratio

As shown in **Figure 8**, as a follow-up chemical reaction occurs faster, both anodic and cathodic half-peak-width decreases (i. e., become sharper), but cathodic one become sharper than the anodic one at a higher rate, resulting in an increase in the half-peak ratio of larger than 1 as illustrated in the **Figure 8**.

$$W_{1/2}^c < W_{1/2}^a < W_{1/2}^a(\text{rev}) = W_{1/2}^c(\text{rev}) = 63/n \text{ (mV)} \quad (67)$$

$$W_{1/2}^a/W_{1/2}^c > 1.00$$

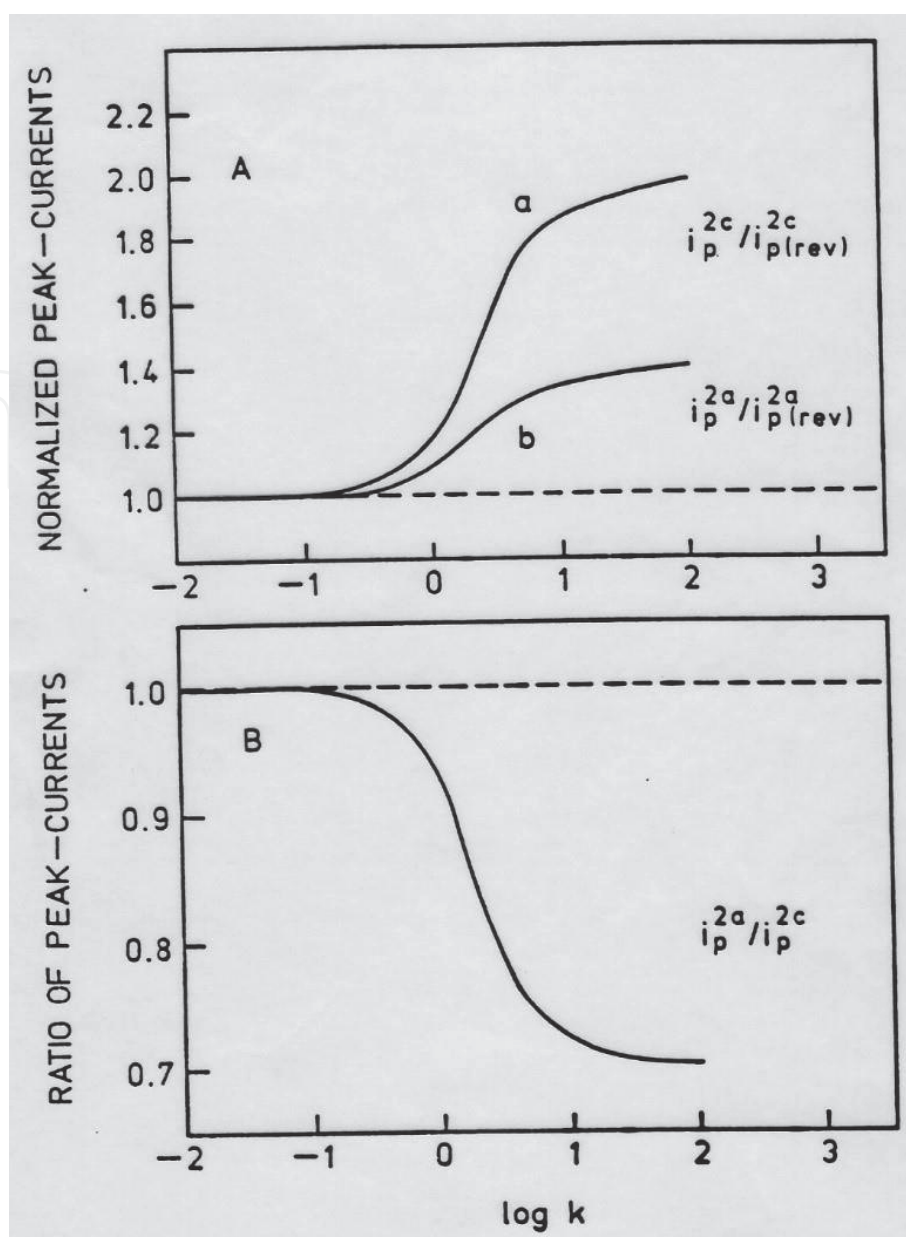


Figure 7. Effect of k (A) on the (a) the anodic, (b) cathodic peak currents of the second derivative, which are normalized with respect to the values of reversible process. (B) Effect of k on the ratio of the anodic to cathodic peak current ratio, i_p^{2a}/i_p^{2c} .

This suggests that the homogeneous rate constant, k , can be directly determined from the measurements of a ratio of the two half-peak-width of the second derivatives.

3.1.4.4 For the third derivative

Third derivatives can be also analyzed graphically in the same fashion, and the details of the graphic analysis and descriptions can be found elsewhere [14]. Only key results are summarized in **Table 2** for the various symmetry parameters, and **Table 4** for key parameters of ratios (several peak-current ratios, half-peak ratios, peak separations or their ratios).

3.2 Advantages of derivative voltammetric method

The scheme of derivative voltammetric (DV) approach is simpler, more straight-forward and faster compared with other methods of studying electrode reaction mechanisms, namely, CV [1, 38–41] and CSWV [66–70]. The present DV

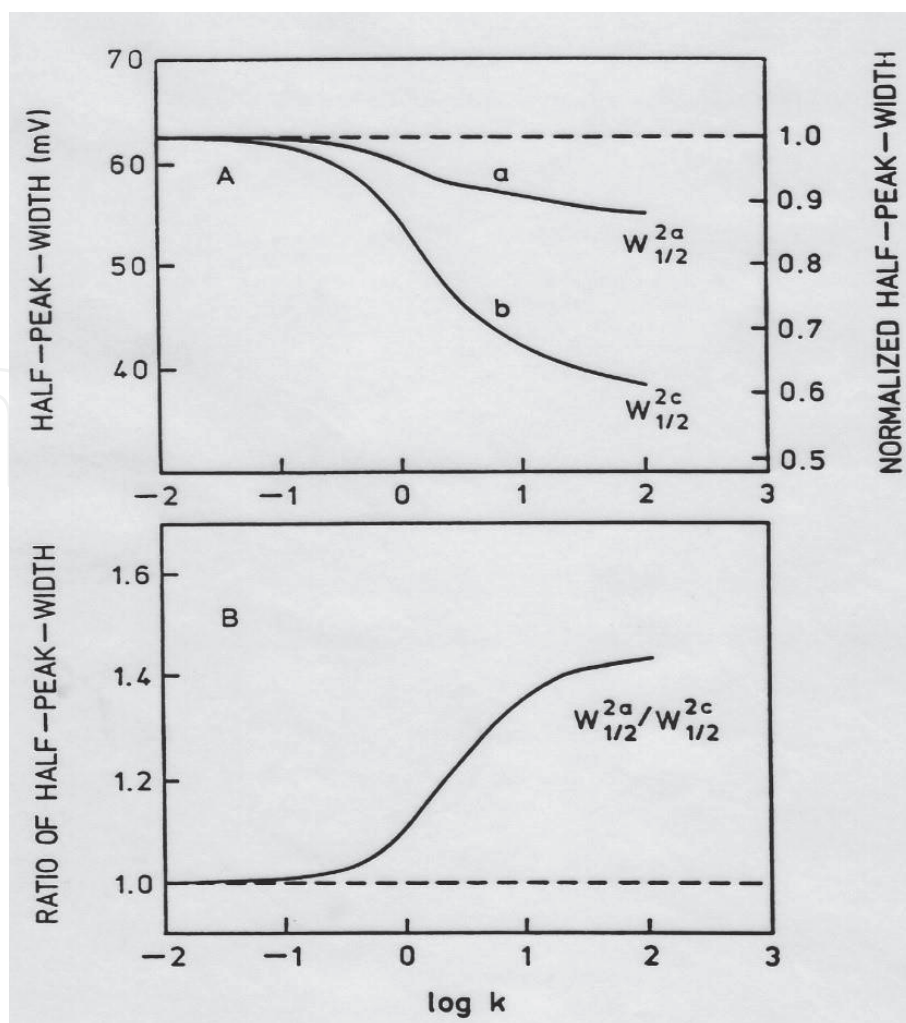


Figure 8. Effect of k (A) on the (a) the anodic, (b) cathodic half peak-widths of the second derivative, on those values normalized to the values for the reversible case whose scales are given at the right side, (B) on the anodic to cathodic half-peak ratios, $W_{1/2}^{2a}/W_{1/2}^{2c}$.

only requires, in general, a single scan for a system under investigation: few experimental variables need to be changed although some experimental variables (such as duration of the pulse) can be optimized at an initial stage of measurement. Mostly, a single scan at a optimized condition will suffice while other methods such as CV and CSWV requires multiple scans (mostly six or more). In present DV method, analysis of the second derivative can be enough for most cases: however, for a system requires a better resolution and a higher sensitivity, one may resort to the third derivatives for more diagnostic parameters.

4. Conclusions

A quantitative measure of symmetry in the original current are not readily available, can be found indirectly from a ratio of difference in several potentials defined from a voltammogram: namely, a quarter-wave potentials ($E_{1/4}$), half-wave potentials ($E_{1/2}$) and a three-quarter-wave potentials); then a ratio of an anodic to cathodic quarter-wave potential differences (i.e., $\Delta E_q^a/\Delta E_q^c = (E_{1/2}-E_{1/4})/(E_{1/2}-E_{3/4})$) is very limited. Nevertheless, the ratio is unity for a symmetrical curve (for a reversible case), but it deviates from one if the curve becomes asymmetrical, yielding 1.14 for E_{irr} (Table 2). On the other hand, asymmetry in first derivatives is more readily found in terms of a ratio of anodic-to-cathodic quarter-peak ratio (W_q^a/W_q^c): this

ratio increases from 1.00 (for E_{rev}) to 1.27 for E_{irr} . The anodic and cathodic parts of the peak-width (W_q and W_q^c) in the first derivative can be more conveniently measured than three potentials (i.e., $E_{1/4}$, $E_{1/2}$ and $E_{3/4}$) in the zeroth derivative; in addition, the change of the ratio in the first derivative is more sensitive than the ratio in the zeroth derivatives (namely, 27% vs. 14%).

In the second and third derivatives, compared to first derivatives, asymmetry in the peak shape is more pronounced, and more than one symmetry parameters are readily obtained, which are given in terms of ratios of different peak-heights, and peak-widths, and peak-potentials; these parameters are based on peak heights (i_p^a and i_p^c) as well as peak widths ($W_{1/2}^a$ and $W_{1/2}^c$) and peak potentials (E_p and E_p). Thus, symmetry ratios of i_p^{2a}/i_p^{2c} , $W_{1/2}^{2a}/W_{1/2}^{2c}$ and $\Delta E_p^{2a}/\Delta E_p^{2c}$ are introduced for second derivatives, and i_p^{3a}/i_p^{3c} , $W_{1/2}^{3a}/W_{1/2}^{3c}$, and $\Delta E_p^{3a}/\Delta E_p^{3c}$ for third derivative (in Tables 2 and 4). All of these values become unity (1.00) for the reversible processes, indicating the symmetry in the curves; but they become no longer unity for quasi-reversible/irreversible electron transfer [15] or chemically coupled processes as the shapes become asymmetrical [12–14, 34] The results are summarized in Tables 2 and 4 with all types of types of processes included. Basically, all of the symmetry parameters for 0th ($\Delta E_q^a/\Delta E_q^c$), for the 1st derivative (W_q^{1a}/W_q^{1c}), and for 2nd derivative (i_p^{2a}/i_p^{2c} , $W_{1/2}^{2a}/W_{1/2}^{2c}$, & $\Delta E_p^{2a}/\Delta E_p^{2c}$) and for third derivative (i_p^{3a}/i_p^{3c} , $W_{1/2}^{3a}/W_{1/2}^{3c}$, $\Delta E_p^{3a}/\Delta E_p^{3c}$) are unity for E_{rev} , they become no longer unity for E_{irr} , $E_{\text{quasi-rev}}$ and two chemically coupled processes of CE_{rev} and $E_{\text{rev}}C$. With the third derivatives, there are also minor symmetry parameters associated with the middle peak with values of 0.32 for the two peak-height ratios (i_p^{3a}/i_p^{3m} and i_p^{3c}/i_p^{3m}) and 1.32 for the two peak-width ratios ($W_{1/2}^{3a}/W_{1/2}^{2m}$, and $W_{1/2}^{3c}/W_{1/2}^{3m}$) for reversible but these ratios are not as simple as the major ones, but changes to 0.22, 0.53, and 1.62 and 0.98 respectively for irreversible case.

5. Summary

From careful analysis of derivatives of voltammetric current-potential curves, it is possible to extract various parameter which are associated with asymmetry of the derivatives associated with various types of electrode mechanisms. Among those parameters, some of them are strongly influenced by electron transfer kinetics and electrode reaction mechanisms associated with a system, and particularly useful in elucidating the reaction mechanisms. In particular, the ratios of the anodic to cathodic peak-currents (i_p^a/i_p^c), and the ratios of the anodic to cathodic peak-widths ($W_{1/2}^a/W_{1/2}^c$) and the ratio of the difference in the anodic and cathodic peak potentials ($\Delta E^a/\Delta E^c$) or the anodic and cathodic peak potential difference ($\Delta E^a - \Delta E^c$) are most sensitive and useful when a simple reversible electron system is disturbed other kinetics, breaking the symmetry in the derivatives. The parameters of each particular systems respond differently to each type of electrode process; thus analysis of symmetry parameters can provide much insight to the mechanistic nature of electrochemical systems. A useful master table for such a diagnostic criteria for differentiating several common types of electrode mechanisms is devised and presented.

Acknowledgements

Several parts of the work have been presented at various conferences including the 3rd Chemical Congress of North America (Toronto, Canada, 1988), the 57th Georgia Academy of Science Meeting (Lawrenceville, GA 1999), the 221st National

Meeting of American Chemical Society (ACS, San Diego, 2001), and the 65th South East Regional Meeting (SERM of ACS, Atlanta, GA 2013). This work was partially supported by Academic Computing Services of Old Dominion University, and with Computer Services through Cornell National Super Computer Center (NSF supported), and by Faculty Fellowship Awards (2008-2009) from the Writers Institute of Georgia Perimeter College (GPC). The author acknowledges the work of all collaborators, Prof. Tae-Kee Hong (Haseo University, Korea) in particular. GPC has been consolidated to Georgia State University (GSU) as Perimeter College in 2016.

IntechOpen

IntechOpen


Author details

Myung-Hoon Kim

Department of Physical Sciences, Perimeter College, Georgia State University,
Dunwoody, USA

*Address all correspondence to: mkim124@gsu.edu

IntechOpen

© 2021 The Author(s). Licensee IntechOpen. This chapter is distributed under the terms of the Creative Commons Attribution License (<http://creativecommons.org/licenses/by/3.0>), which permits unrestricted use, distribution, and reproduction in any medium, provided the original work is properly cited. 

References

- [1] A. M. Bond, *Modern Polarographic Methods in Analytical Chemistry*, Marcel Dekker, New York (1980) 145–157, 212–216, 288–389.
- [2] T. C. O’Haver, and G. L. Green, *Anal. Chem.*, **48** (1976) 312.
- [3] A. F. Fell, *Trends in Analytical Chemistry*, **2** (1983) 63–66.
- [4] S. V. Romanenko, *J. Anal. Chem.*, **52** (1997) 822–896.
- [5] K. Nagashima, M. Matsumoto, and S. Suzuki, *Anal. Chem.*, **57** (1985) 2065–2067.
- [6] D. L. Roelke, C. D. Kennedy, and A. D. Weidemann, *Gulf Mex. Sci.*, **2** (1999) 75–86.
- [7] R. Mehrotra, G Tyagi, D.K. Jangir, R. Dawar, and N. Gupta, *J. Ovarian Cancer*, **3** (2010) 27.
- [8] M. I. Toral, N. Lara, J. Gomez, and P. Richter, *Anal. Lett.*, **35** (2002) 153–166.
- [9] A. P. Kumar, P.R. Reddy, and V. K. Reddy, *J. Anal. Chem.*, **63** (2008) 26–29.
- [10] V. D. Parker, *Electroanalytical Chemistry*, A.J. Bard, Editor, Vol. 14, Marcel Dekker, New York (1986) p28.
- [11] M.-H. Kim, *Anal. Chem.*, **59** (1987) 2136–2144.
- [12] M.-H. Kim, *Anal. Sci. Tech. (J. Korean Soc. Anal. Sci.)*, **2** (1989) 225–236.
- [13] M.-H. Kim, V. P. Smith and T.-K. Hong, *Bull. Korean Chem. Soc.*, **11** (1990) 497–505.
- [14] M.-H. Kim, *J. Electrochem. Soc.*, **137** (1990) 3815–3825.
- [15] M.-H. Kim, V. P. Smith and T.-K. Hong, *J. Electrochem. Soc.* **140** (1993) 712–7215.
- [16] J. Gonzales. Molina, M. Lopez-Tenes, and C. Serna, *J. Electrochem. Soc.* **147** (2000) 3429–3435.
- [17] A. Molina, J. Gonzales, and M. M. Moreno, *Electroanalysis*, **14** (2002) 281–291.
- [18] A. Molina, and I. Morales, *Int. J. Electrochem. Sci.*, **2** (2007) 386–405.
- [19] Y. P. Ding, W. L. Liu, Q. S. Wu, and X. G. Wang, *J. Electroanal. Chem.*, **575** (2005) 275–280
- [20] J. Mbindyo, L. Zhou, Z. Zhang, J. D. Stuart, and J. E. Rusling, *Anal. Chem.*, **72** (2000) 2059–2065
- [21] A. Murthy, and A Manthiram, *J. Phys. Chem. C*, **116** (2012) 3827–3832.
- [22] M. Lovric, J. J. O’Dea, and J. Osetryoung, *Anal. Chem.*, **55** (1983) 704–708.
- [23] C. G. Chan, and J. Kelly, *Earthquake Engineering & Structural Dynamics*, **19** (1990) 220–241
- [24] C. L. Vaughn, *Int. J. Biomedical Computing*, **13** (1980), 375–386
- [25] H. J. Woltring, *Adv. Eng. Software*, **8** (1986), 104–113.
- [26] G. Ferrigno, and M. D’Amico, *J. Biomechanics*, **22** (1989), 1010.
- [27] G. Giakas, and V. Baltzopoulos, *J. Biomechanics*, **30** (1997), 851–855.
- [28] A. M. Zoubiv, M. Viberg, R. Chellappa, and S. Theodoridis, in *Academic Press Library in Signal Processing, Vol. 3 Array and Statistical Signal Processing*, Amsterdam (2014).
- [29] M. Jakubowska, *Electroanalysis*, **23** (2011), 553–572.

- [30] L. Meitis, *Polaographic Techniques*, 2nd Ed., John Wiley & Sons, New York (1965), p 114, 418, 457.
- [31] M.-H. Kim, and T.-K. Hong, *Georgia J. Science*, **57**(1999), 46.
- [32] T-K Hong, I. Rusodimos, and M.-H. Kim, *J. Electroanal. Chem.*, **785**(2017), 255–264.
- [33] G. Giakas, and L. Stergiolas, and A. Vourdas, *J. Biomechanics*, **33** (2000), 567–574.
- [34] T. C. O'Haver and T. Begley, *Anal. Chem.*, **53** (1981) 1876–1878.
- [35] A. Cobelo-Garcia, J. Santos-Echeandia, D. E. Lopez-Sanchez, C. Amecija, and D. Omanovic, *Anal. Chem.*, **86** (2014) 2306–2313.
- [36] A. P. Murthy, K. Duraimurugan, J. Sridar, and J. Madhavan, *Electrochim. Acta*, **317** (2019), 182–190.
- [37] G. Ziyatidinova, E. Yacupova, E. Ziganshina, and H. Budnikov, *Electroanalysis*, **31** (2019) 2130–2137.
- [38] A. J. Bard, and L. Faulkner, *Electrochemical Methods and Applications*, 2nd Ed. John Wiley & Sons, New York (2000).
- [39] N. Elgrishi, K. J. Rountree, B. D. McCarthy, E. S. Rountree, T. T. Eisenhart, and J. L. Dempsey, *J. Chem. Educ.*, **95** (2018) 197–206.
- [40] P. T. Kissinger, and W. R. Heineman, *Laboratory Techniques in Electroanalytical Chemistry*, 2nd Ed., Dekker, Monticello, NY (1996).
- [41] D. K. Gosser, *Cyclic Voltammetry: Simulation and Analysis of Reaction Mechanisms*, VCH, New York, NY (1993).
- [42] M.-H. Kim and V.P. Smith, *Anal. Sci. Tech. (J. Korean Soc. Anal. Sci.)* **2** (1989) 237–245.
- [43] K. B. Oldham, and J. Myland, *Fundamentals of Electrochemical Sciences*, Academic Press, New York (2012), p 434–435.
- [44] D. D. Macdonald, *Transient Techniques in Electrochemistry* Plenum Press, New York (1977) p76.
- [45] M. L. Olmstead and R.S. Nicholson, *J. Electroanal. Chem.*, **14** (1967) 133–141.
- [46] J. Galvez, A. Molina, and T. Fuente, *J. Electroanal. Chem.*, **107** (1980) 217–231.
- [47] J. Galvez, M. L. Alkaraz, T. Perez, M. L. Cordova, *Anal. Chem.*, **57** (1985) 2116–2120.
- [48] J. Galvez, *Anal. Chem.*, **57** (1985) 585–591.
- [49] J. Galvez, A. Molina, C. Serna, and R. Saura, *J. Electroanal. Chem.*, **119** (1986) 37–45.
- [50] J. Goodisman, *J. Electroanal. Chem.*, **114** (1983) 33–43.
- [51] F. Martinez-Oritz, M. L. Alkaraz, I. Roca, and M. Lopez-Tenes, *J. Electroanal. Chem.*, **443** (1998) 243–252.
- [52] A. Molina, C. Serna, and F. Martinez-Oritz, *J. Electroanal. Chem.*, **486** (2000) 9–15.
- [53] C. Serna, A. Molina, M. M. Moreno, and M. Lopez-Tenes, *J. Electroanal. Chem.*, **546** (2003) 97–108.
- [54] M. Lovric, and Y.I. Tur'yan, *Croatia Chem. Acta*, **76** (2003) 189–197.
- [55] F. Martinez-Oritz, M. L. Alkaraz, and I. Roca, *J. Electroanal. Chem.*, **568** (2004) 79–86.
- [56] A. Molina, F. Martinez-Oritz, E. Laborda, R. G. Compton, *Electrochim. Acta*, **55** (2010) 5163–5172.

- [57] R. L. Birke, M.-H. Kim and M. Strassfeld, *Anal. Chem.*, **53** (1981) 852–856.
- [58] M.-H. Kim and R. L. Birke, *Anal. Chem.*, **55** (1983) 522–527.
- [59] M.-H. Kim and R. L. Birke, *Anal. Chem.*, **55** (1983) 1735–1741.
- [60] M.-H. Kim, L. Yan, M.-Z. Czae, and R. L. Birke, *Electroanalysis*, **15** (2003) 1541–1553.
- [61] M.-H. Kim and R. L. Birke, *Proceedings of the Korean Federation of Science and Technology: 11th Biennial Meetings, Physical Sciences Section, Korea University*, (1990) 606–610.
- [62] J. J. O’Dea, J. Osteryoung, and R. A. Osteryoung, *Anal. Chem.*, **53** (1981) 695–701.
- [63] J. G. Osteryoung and R. A. Osteryoung, *Anal. Chem.*, **57** (1985) 101A–110A.
- [64] J. J. O’Dea, and J. Osteryoung, *Anal. Chem.*, **85** (1993) 3090–3097.
- [65] L. Ramaley, and M. S. Klause, *Anal. Chem.*, **41** (2002) 1632–1635
- [66] J. C. Helfrick, and L. A. Bottomley, *Anal. Chem.*, **81** (2009) 9041–9047.
- [67] M. A. Mann, C. Helfrick, and L. A. Bottomley, *Anal. Chem.*, **86** (2014) 8183–8191.
- [68] J. C. Helfrick, M. A. Mann, and L. A. Bottomley, *Electrochim. Acta*, **205** (2016) 20–28.
- [69] M. A. Mann, J. C. Helfrick, and L. A. Bottomley, *J. Electrochem. Soc.*, **163** (2016) H3101–H3109.
- [70] J. C. Helfrick, M. A. Mann, and L. A. Bottomley, *ChemPhysChem*, **17** (2016) 2596–606.
- [71] Eduardo Laborda, José María Gómez-Gil, Manuela López-Tenés, and Angela Molina, *J. Electroanal. Chem.*, **873** (2020), 114421 (<https://doi.org/10.1016/j.jelechem.2020.114421>).
- [72] J. R. Delmastro and D. E. Smith, *Anal. Chem.*, **38** (1966) 169–179.
- [73] A. Molina and J. Gonzalez, *Pulse Voltammetry and Physical Chemistry and Electroanalysis*, Springer, Heidelberg, (2016) p155.